Journal of Civil Engineering, Science and Technology
Volume 12, Issue 2, September 2021

LAND SURFACE TEMPERATURE (LST) ESTIMATION AT KUSHTIA DISTRICT, BANGLADESH

Md. Jahir Uddin*, Faisal Jahangir Swapnil
Department of Civil Engineering, Khulna University of Engineering & Technology, Khulna, Bangladesh

Date received: 21/01/2021 Date accepted: 17/09/2021
*Corresponding author's email: jahiruddin@ce.kuet.ac.bd
DOI: 10.33736/jcest.3985.2021

Abstract — Land Surface Temperature (LST) is a key phenomenon in worldwide climate change. The knowledge of surface temperature is important to a range of issues and themes in earth sciences, central to urban climatology, global environmental change, and human-environment interactions. In this study, LST for Kushtia District, Khulna division, Bangladesh, is derived using Arc-GIS software version from the images of Landsat 8 Optical Land Imager (OLI) of 30 m resolution and Thermal Infrared Sensor (TIR) data of 100 m resolution, Landsat-7 Enhanced Thematic Mapper plus (ETM+) with opto-mechanical sensor and Spatial Resolution of 30 m (60 m – thermal, 15-m panchromatic) and Landsat-5 Thematic MAPPER (TM) satellites. A total time span of 20 years, starting from 1998 to 2018 is selected. At every 5 years interval starting from 1998, air temperature, LST, Normalized Difference Vegetation Index (NDVI) and Normalized Difference Water Index (NDWI) have been calculated. Using the equation from Landsat user's handbook, the digital number of thermal infrared band is converted into spectral radiance. Plank's Inverse Function is used to obtain the effective at-sensor brightness temperature from the spectral radiance. The surface emissivity based on NDVI classes is used to retrieve the final LST. The study reveals that LST is increasing with the passage of time. Maximum values of LST are found along the North-East and North-West regions of Kushtia district. NDVI is found to have positive correlation with LST. Also, it has been found that NDWI has little influence on LST. The reasons behind the rise and fall of LST in different years are explained from changes in total vegetation coverage and total abundance of water body coverage viewpoint. The spatial distribution figures of air temperature, LST, NDVI and NDWI could be used as a guideline for urban planning, strategies for quality improvement of urban environment and a smart solution to the reduction of LST.

***Keywords*:** Land Surface Temperature, Vegetation, Water body, Estimation, Kushtia district

1.0 INTRODUCTION

LST as a key indicator of the earth surface energy budget is broadly needed in the applications of hydrology, meteorology, and climatology. It is crucial significance to the net radiation budget at the soil surface and to check the state of crops and vegetation, as well as a critical marker of both the nursery impact and the vitality flux between the climate and ground. The assessment of LST used for a country like Bangladesh is a feasible way to connect its seasonal features with changing meteorological conditions. LST is impacted by the characteristics of the land surface such as vegetation cover and its sort, land-use cover and surface imperiousness. Ceaseless urbanization has come about into expanding within the urban zone and it has caused critical changes within the land surface. The LST can give critical data approximately the surface physical properties and climate which feature a key part in various environmental forms [1].

LST is the temperature emitted by the land surface and is dignified in kelvin or Celsius [2]. This one is prominently exaggerated by increasing Green-House Gases in the atmosphere. As per it increases, it liquefies the glaciers and ice pieces in the polar zone. Therefore, it leads to flood, sea level rises and related natural calamities. Rise in LST also affects the climatic condition of the monsoon countries leading to erratic precipitation [3]. Thus, the vegetation in the entire earth surface is affected and LST is generally dependent on vegetation, particularly healthy vegetation, build-up or barren area and water body. Estimation of a LST area was hard before the creation of Earth Observation Satellites (EOS) [4]. Usually, the calculation of LST was done for a specific set of sample points and were interpolated into isotherms to generalize the point data into area data [5]. By using different spatial interpolation methods the most isometric LST maps were interpolated from the measurements at sample locations [6]. The author proves in their research that type of land use; changes of land cover have significant impact on LST [7]. Other than, the effect of urban growth spatial pattern on LST has been highlighted by [8]. Once more, the effect of forest on

LST has been revealed by [9]. Thus, there are large numbers of researches works on land covering that effects LST. Satellite images are used which contain information of land covering and pattern such as vegetation, water body, bare soil etc., even it is useful to analyze terrain effect on land surface [10].

Presently with the coming of satellites and high determination sensors, it is feasible to measure LST spatially. It can be calculated for an area at a stretch with the usage of thermal ultraviolet bands supplied by Landsat satellite. A number of researchers had used the Landsat imageries to develop land use or cover images. Due to tall heterogeneity of land surfaces and the challenges in expelling air impacts, remotely sensing land surface is very challenging. Besides, there's a bungle between remote sensing and land surface model requirements such as remote sensing measures ghastly emissivity through channels on certain wave-lengths [11]. Nonetheless land surface models needed broadband emissivity for the calculation of upward long wave radiation and by using the Stefan–Boltzmann law. Due to atmospheric absorption, only the spectral radiance within the infrared water vapor window region (8 to14 μm) is measured using Thermal Infrared Remote Sensing. These measurements are needed because of broadband emissivity. Depending on the number of bands used, the LST may be recovered as of thermal images by Single Infrared Channel Method or by the Split Window Method [12]. LST had been used for an extensive diversity of scientific research [13]; [14] and was a significant parameter for computing surface urban heat islands, for estimating building energy consumption and also for evaluating heat related menaces [15]; [16]; [17]; [18]. This one was sensitive to different land surface features and therefore can be used to excerpt data on diverse land use or cover types [19]. Significant LST variations over various land use or cover types in “English Bazar Municipality”, for the District of Malda at West Bengal in India had been observed by Pal and Ziaul [20]. The urbanization has found as the key driving factor for land cover changes and subsequently increase of LST and the stable growth of LST can disrupt the ambient habitation for the human beings and other ecosystem followers. The LST was also suggested for the assessment of drought providing the surface temperature information about an area [21].

The LST can be a stimulating field for many researchers in Bangladesh. Bangladesh is also facing adverse effects of global warming with the quick increasing of industries and urbanization. LST provides information about the variant of ground surface temperature with the passageway of years. Thus, in this case, LST can be an indication for the extent of global warming and green house.

Although there are a number of vegetation indices, one of the most commonly used is the NDVI. The NDWI is known to be strappingly associated to the plant water content. It is thus a very good proxy for plant water stress. It is a real time retrieval of soil moisture, which has high retrieval accuracy [9]. Initially water stress is caused by drought or high soil salinity [10]. NDWI is an important indicator of detecting drought like catastrophe, as [11] say that it is caused by long-term lack of soil water content which would affect agriculture, ecology and socioeconomic; it is predominantly harmful to food production as well. According to [12] the urban area is a small fraction of the earth's surface area but has a disproportionate influence on its surroundings. Mapping urban area in an accurate and regular manner is essential for different planning applications such as watershed run-off prediction. Researchers akin to [15] and [16] have similar perspective that remote sensing images are helpful for monitor the spatial distribution and growth of urban built-up areas because of their ability to provide timely and synoptic views of land area.

This study contains several objectives such as determination of LST changes over Kushtia district for a time period of 20 years using Landsat satellite images and Arc-GIS software and also determination of NDVI and NDWI of Kushtia district over the mentioned time period and investigation the impact of water body (NDWI) and vegetation (NDVI) on LST. Amongst the major scopes the study gives a comprehensible thought of the changing pattern of LST of Kushtia district over 20 years of time period and provides an opportunity to estimate the quantity of land surface area covered by vegetation and water bodies. In addition, it makes it possible to calculate the percentage of area occupied or loss by vegetation and water bodies or similar type of features.

Therefore, it has become indubitably necessary to calculate LST and examine the relationship between vegetation and land surface temperature (LST) of Kushtia city and find out its consequences in the future.

1.1. Study Area

Kushtia district comprises of 6 sub-districts (shown in Figure 1) situated in the Khulna Administrative Division of Western Bangladesh. DMS (Degrees Minutes Seconds) latitude longitude coordinates for Kushtia are: 23°54'10.08"N, 89°7'9.95"E. The Kushtia district is surrounded by Rajshahi, Natore, Pabna districts to the North;

by Chuadanga, Jhenaidah districts to the South; by Rajbari district to the East; and by West Bengal and Meherpur districts to the West and has an area of 1608.80 km^2. The main rivers flowing through Kushtia are Ganges, Goṛai-Modhumoti, Mathabhanga, Kaligonga, and Kumar etc. The average high and low temperature is 37.8°C and 9.2°C respectively, and average annual rainfall is 1467mm. The land areas of upazilla's of Kushtia: Kushtia 42.79km^2, Kumarkhali 11.00km^2, Bheramara 10.00km^2, Mirpur 9.22 km^2 and Khoksa12.38 km^2. Both agriculture and industries are key dependable factor for the economy of Kushtia.

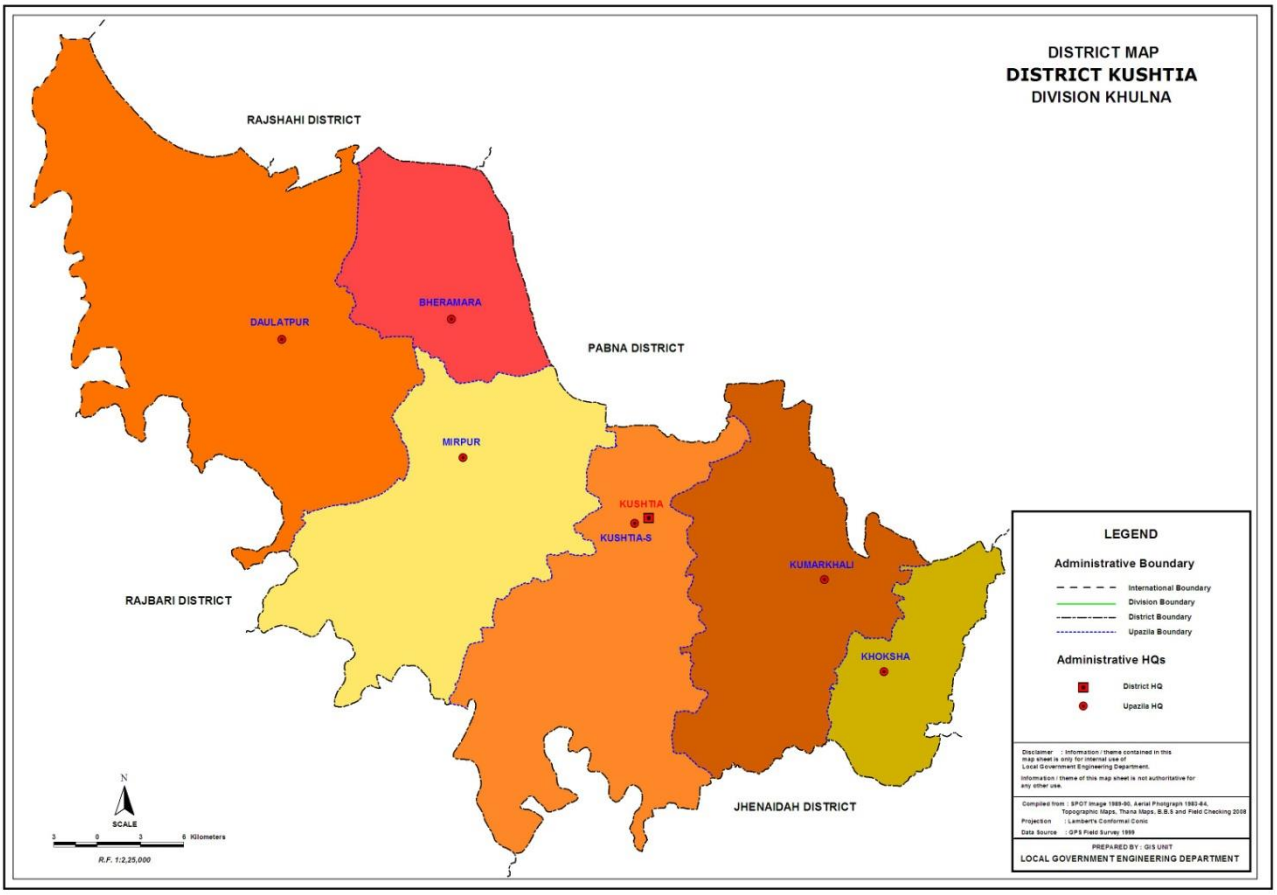

Figure 1 Local Government Engineering Department (LGED) map of Kushtia

2.0 METHODOLOGY

Shape files of Kushtia District were extracted from https://www.google.com/earth (Google Earth) and through a collection of satellite images of years 1998, 2003, 2008, 2013 and 2018 from https://earthexplorer.usgs.gov (USGS Earth Explorer) and https://glovis.usgs.gov (USGS Global Visualization Viewer). The gap filling of satellite images for years 2008 and 2013 were done using ERDAS IMAGINE-2014. Atmospheric temperature, LST, NDVI and NDWI of Kushtia District were calculated with the aid of Arc-Tool Box, which is a central application of Arc-Map 10.5. Areas covered by vegetation, water-body and other type features according to NDVI and NDWI were computed.

2.1 Collection and Processing of Satellite Images

A total time span of 20 years was considered for this study. Landsat-5 TM images of 1998, Landsat-7 ETM+ images of years 2003, 2008 and 2013 and Landsat-8 OLI and TIRS images of year 2018 at the middle of February at UTM (Universal Transverse Mercator) zone-46 were downloaded. From May 31, 2003, Landsat-7 ETM+ had scan line fault, due to failure of Scan Line corrector (SLC), so the image data type was erroneous. There were some techniques to improve the quality of the images. In this study, ERDAS IMAGINE-2014 software was used for focal analysis to compensate errors. This method was designed to modify neighboring pixels in a single Landsat 7 SLC-off scene, creating a final aesthetic image. This method was designed using ERDAS Imagine 2014™*, along

with ENVI™* or Adobe Photoshop 2017™ * for final filled-image verification. The approximate time to complete a scene was 20 minutes.

2.2 Calculation of Atmospheric Temperature

During 1G-product rendering, image pixels were converted to units of absolute radiance using 32 bit floating-point calculations. Pixel values were then scaled to byte values prior to media output. The following equation is used to convert DN's in a 1 G product back to radiance unit for TM and ETM+:

$$L_\lambda = \left(\frac{LMAX_\lambda - LMIN_\lambda}{QCALMAX - QCALMIN} \right) * \left(QCAL - QCALMIN \right) + LMIN_\lambda \quad (1)$$

Where, L_λ is spectral radiance at the sensor's aperture in watts/(meter squared * ster * μm), *QCAL* is the quantized calibrated pixel value in DN, $LMIN_\lambda$ is the spectral radiance that is scaled to *QCALMIN* in watts/(meter squared * ster * μm), $LMAX_\lambda$ is the spectral radiance that is scaled to *QCALMAX* in watts/(meter squared * ster * μm), *QCALMIN* is the minimum quantized calibrated pixel value (corresponding to $LMIN_\lambda$) in DN, and *QCALMAX* is the maximum quantized calibrated pixel value (corresponding to $LMAX_\lambda$) in DN.

The following equation is used to convert DN's in a 1 G product back to radiance unit for TIRS:

$$L_\lambda = M_L * Q_{cal} + A_L \quad (2)$$

Here,M_L is radiance multiplicative scaling factor for the band (RADIANCE_MULT_BAND_n from the metadata), Q_{cal} is L1 pixel value in DN, and A_L is radiance additive scaling factor for the band (RADIANCE_ADD_BAND_n from the metadata).

ETM+ Band 6 (thermal) and TIRS Band 10 and 11 imagery were converted from spectral radiance to a more physically useful variable. This was the effective at satellite temperatures of the viewed Earth-atmosphere system under an assumption of unity emissivity and using pre-launch calibration constants. The conversion formula is:

$$T = \frac{K2}{\ln\left(\frac{K1}{L_\lambda} + 1 \right)} \quad (3)$$

Where, *T* is brightness temperature (*K*), *K*2 is calibration constant 2, and *K*1 is calibration constant 1.

2.3 Calculation of NDVI

NDVI was calculated from the visible and near-infrared light reflected by vegetation. NDVI can be calculated by the following equation:

$$NDVI = \frac{NIR - VISR}{NIR + VISR} \quad (4)$$

Where, *NIR* is spectral reflectance measurements acquired in the near infra-red regions and *VISR* is spectral reflectance measurements acquired in the visible red regions. A value between -1 and + 1 was generated from the result of this formula. If it had low reflectance (or low values) in the red channel and high reflectance in the NIR channel, this produced a high NDVI value and vice versa.

2.4 Calculation of NDWI

The formula stands for NDWI is given below**:**

$$NDWI = \frac{VISG - NIR}{VISG + NIR} \quad (5)$$

Where, *NIR* is spectral reflectance measurements acquired in the near infra-red regions and *VISR* is spectral reflectance measurements acquired in the visible red regions. This formula generated a value between -1 and +1. If it had low reflectance (or low values) in the red channel and high reflectance in the NIR channel, this yielded a high NDWI value and vice versa.

2.5 Conversion of Atmospheric Temperature to LST

After calculating NDVI for a specific year, it yielded either a positive or a negative NDVI value. Then using the NDVI value, the proportion of vegetation is calculated from the following equation:

$$P_v = \left(\frac{NDVI - NDVI_{MIN}}{NDVI_{MAX} - NDVI_{MIN}} \right)^2 \quad (6)$$

Where, P_v refers to proportion of vegetation.

Then using the value of P_v Land Surface Emissivity (LSE) was also calculated. The knowledge of LSE was necessary to apply the methods of retrieving LST from a Landsat image. An alternative, operative (easy to apply) procedure was to obtain the LSE image from the NDVI of different approaches given in the literature [27]. A modification of the last one had been used, in which the NDVI Thresholds Method (NDVITHM), which showed a good working result. The final expression for calculating emissivity based on this method is:

$$e = 0.004 P_v + 0.986 \quad (7)$$

Where, *e* denotes LSE.

Finally LST is derived using following equation:

$$LST = \frac{T}{1 + \frac{wT}{p} \times \ln(e)} - 273.15 \quad (8)$$

Where, *W* is emitted radiance wavelength (μm), $p=h/s=1.438\times10^{-2}$ mK, *h* is constant of Planck's (6.626×10^{-34} Js), *s* is constant of Boltzmann (1.38×10^{-23} J/K), *c* is light Velocity (2.998×10^{-8} m/s).

3.0 RESULTS AND DISCUSSION

3.1 Land Surface Temperature and Atmospheric Temperature

In Figure 2, graphical comparasion of LST in the years 1998, 2003, 2008,2013 and 2018 is represented.

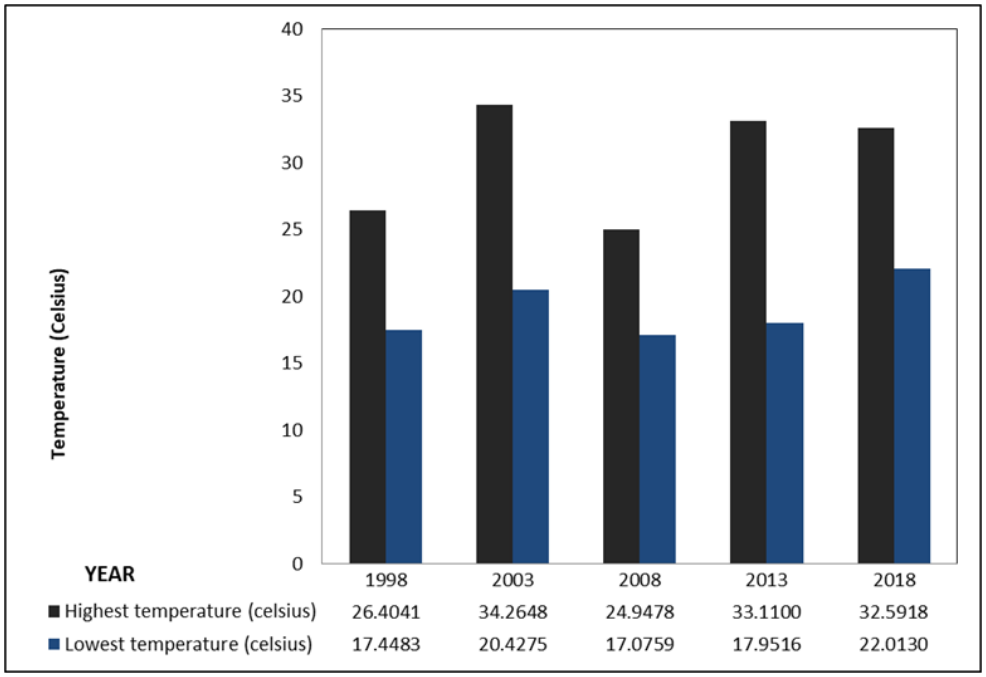

Figure 2 Highest and Lowest LST of different years

It was observed that highest and lowest LST of year 1998 were 26.4041 ^{0}C and 17.4483 ^{0}C. In 2003, LST abruptly rose to 34.2648 ^{0}C and 20.4275 ^{0}C. This was due to the fact that atmospheric temperature during that year also faced a rising pattern which can be spectated from Figure 3. But the most dramatical part to realize was the dramatic drop down of LST in the year of 2008. This was very difficult to understand, the reason of this temperature drop, as due to global warming both atmospheric and LST were expected to face a rising trend. However, in the later section of this study the reason behind this drop down was explained from the basis of relations among NDVI, NDWI and LST. However both in years 2013 and 2018, LST had increased too many folds.

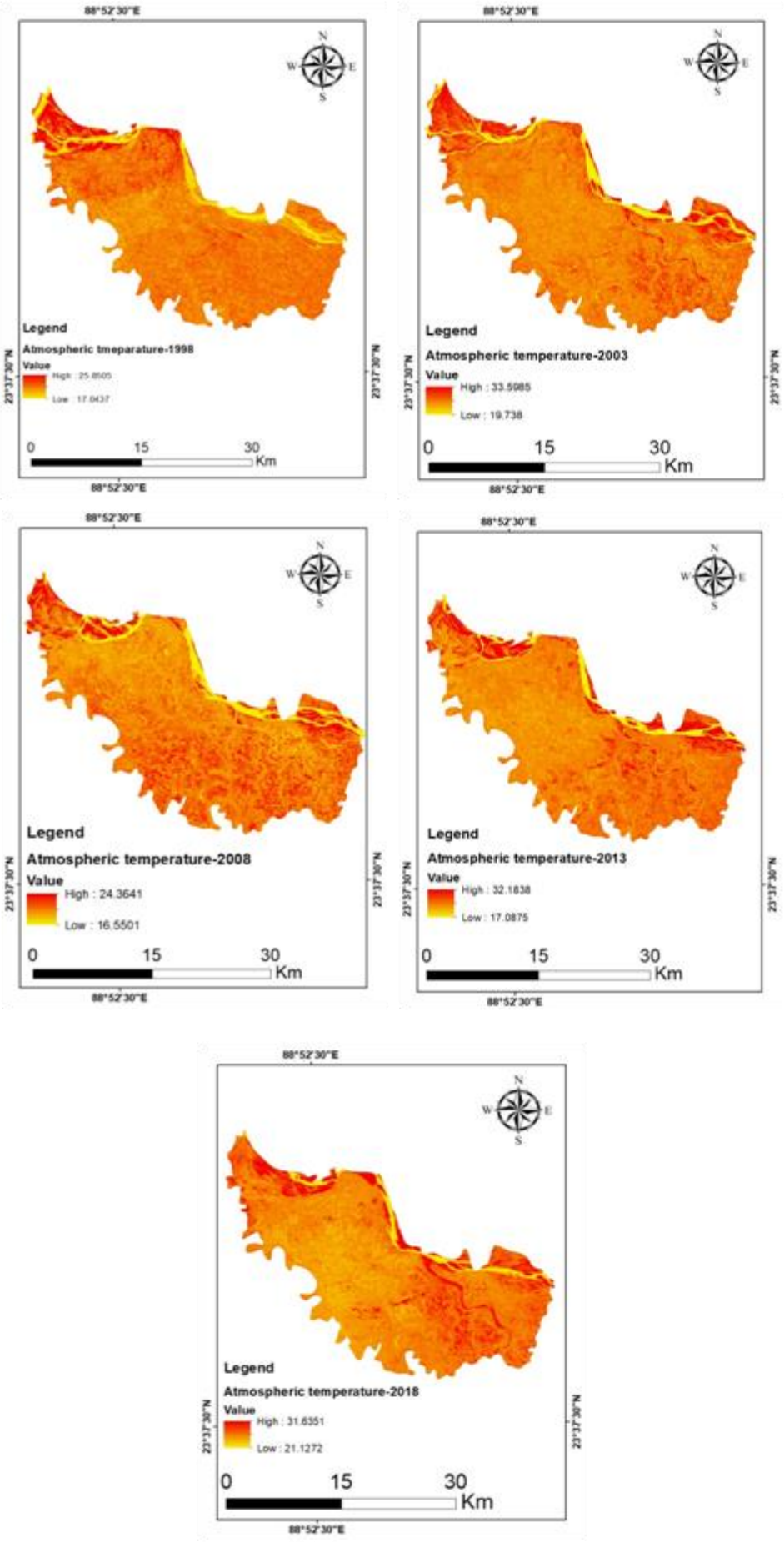

Figure 3 Spatial distribution of atmospheric temperature of years 1998, 2003, 2008, 2013 and 2018

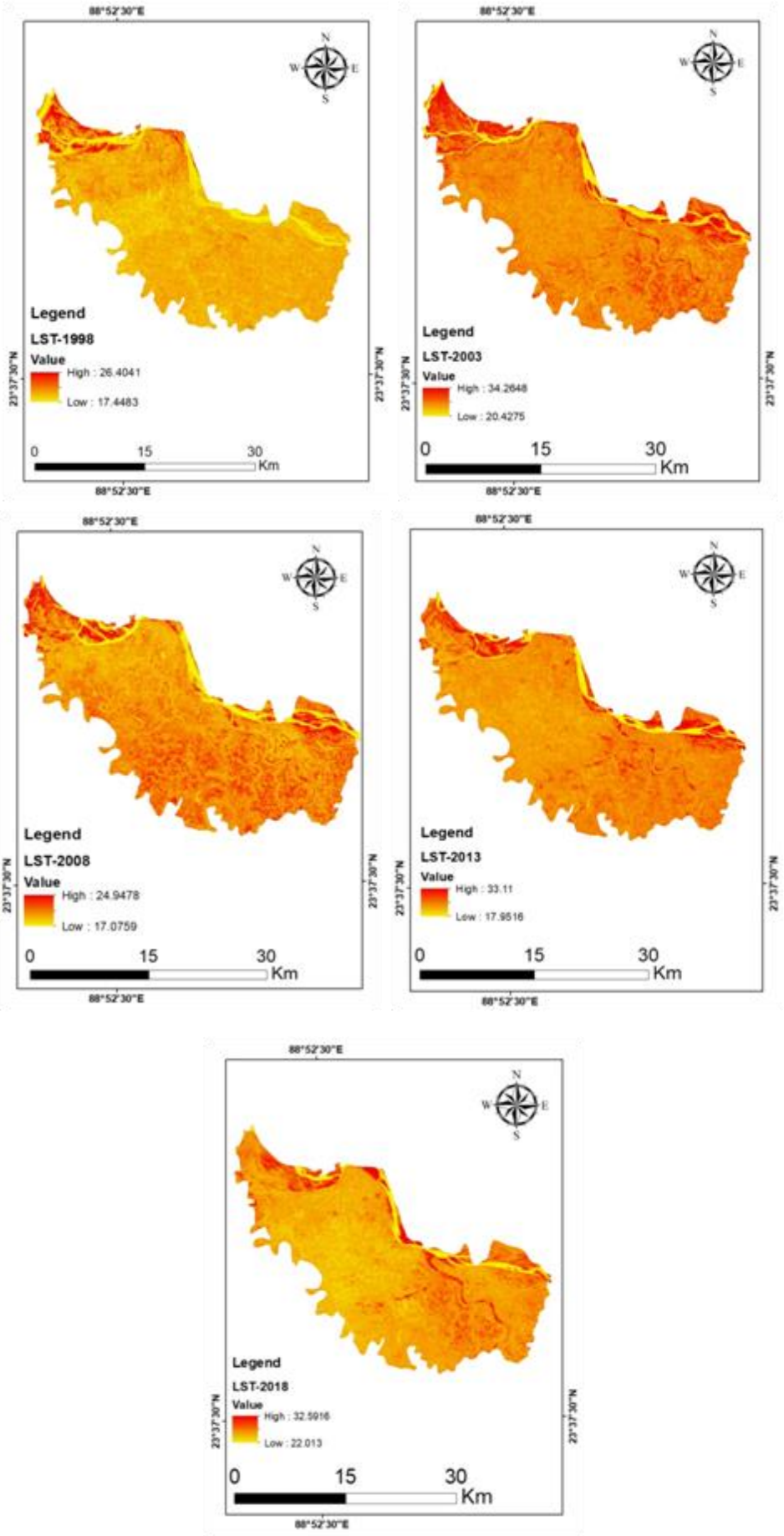

Figure 4 Spatial distribution of LST of years 1998, 2003, 2008, 2013 and 2018

In Figure 4, spatial distributions of highest and lowest LST of Kushtia district had been shown. It can be seen that along the North-East and North-West portion of the area, LST was quiet more than the other regions. River Padma and Gorai had traversed through these portions of the district. For this study images from middle of February were selected. It was found that during that particular time staggering amount of sand spout was available instead of water. So, the river bed got warmer as sand absorbed large portion of heat during midday. As a consequence, LST developed excessively in these areas in comparison with others. LST was low along South-West and South-East areas of Kushtia District. It was because of the presence of healthy vegetation in these areas which is discussed in the later section of this study.

3.2 Normalized Difference Vegetation Index (NDVI)

Spatial distribution of vegetation cover is presented in Figure 5.

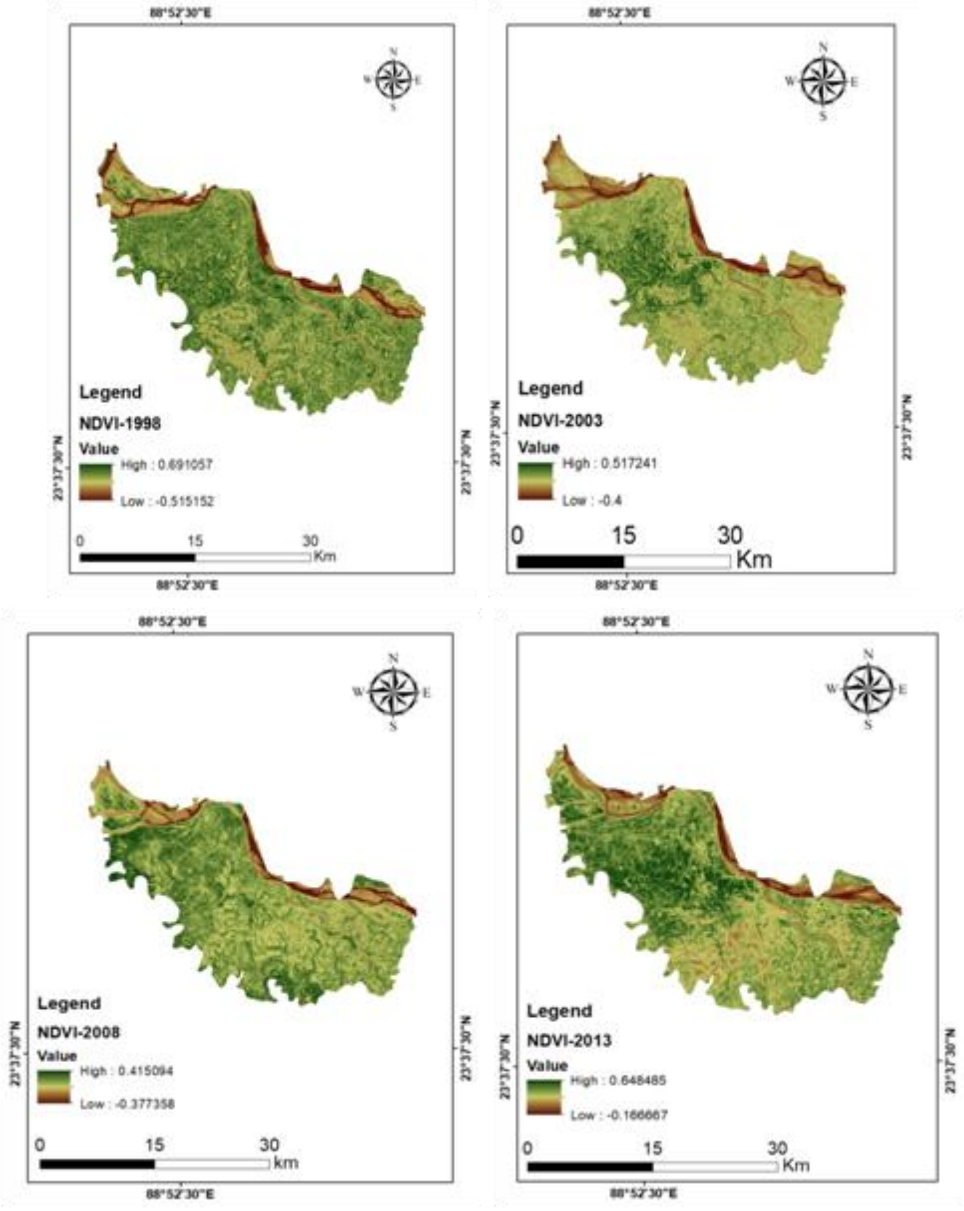

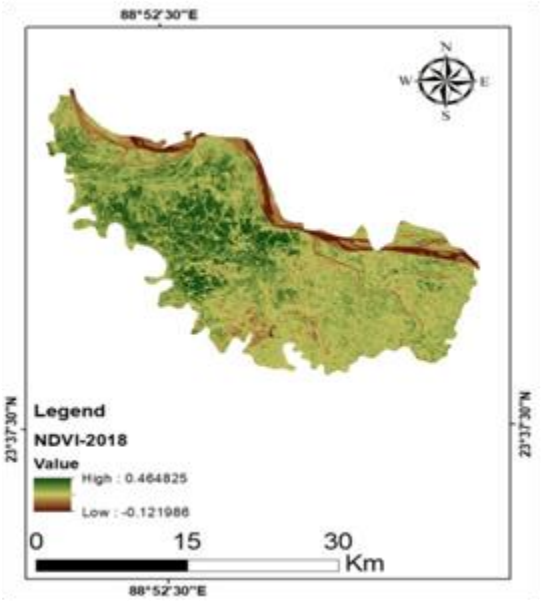

Figure 5 Spatial distribution of NDVI of years 1998, 2003, 2008, 2013 and 2018.

The ranges of highest and lowest values of NDVI for the study years are also shown in Figure 5. Here maximum vegetation (green color) showed maximum coverage in the year of 1998. In year 2003 there was a drop down of maximum NDVI value (0 .517241) which was continued in year 2008. But in year 2013 maximum NDVI value was 0.648485, which was similar to the year 1998. But in year 2013 it decreased again and nearly equivalent to year 2008. The most interesting feature pertaining to the minimum or negative value of NDVI was also maximum in year 1998 (-0.515152) and minimum in year 2018 (-0.121986). From the spatial distribution of vegetation, it was obvious that maximum vegetation covering area lied in North-West portion of the Kushtia district while South-East region having a moderate extent of vegetation. This is exactly that area where LST was found to have lowered values than the others. NDVI value greater than 0.6 that represented healthy vegetation, large tropical forest or tree. Lower positive value meant small bush-like or unhealthy vegetation.

3.3 Normalized Difference Water Index (NDWI)

Spatial distribution of NDWI is presented in Figure 6.

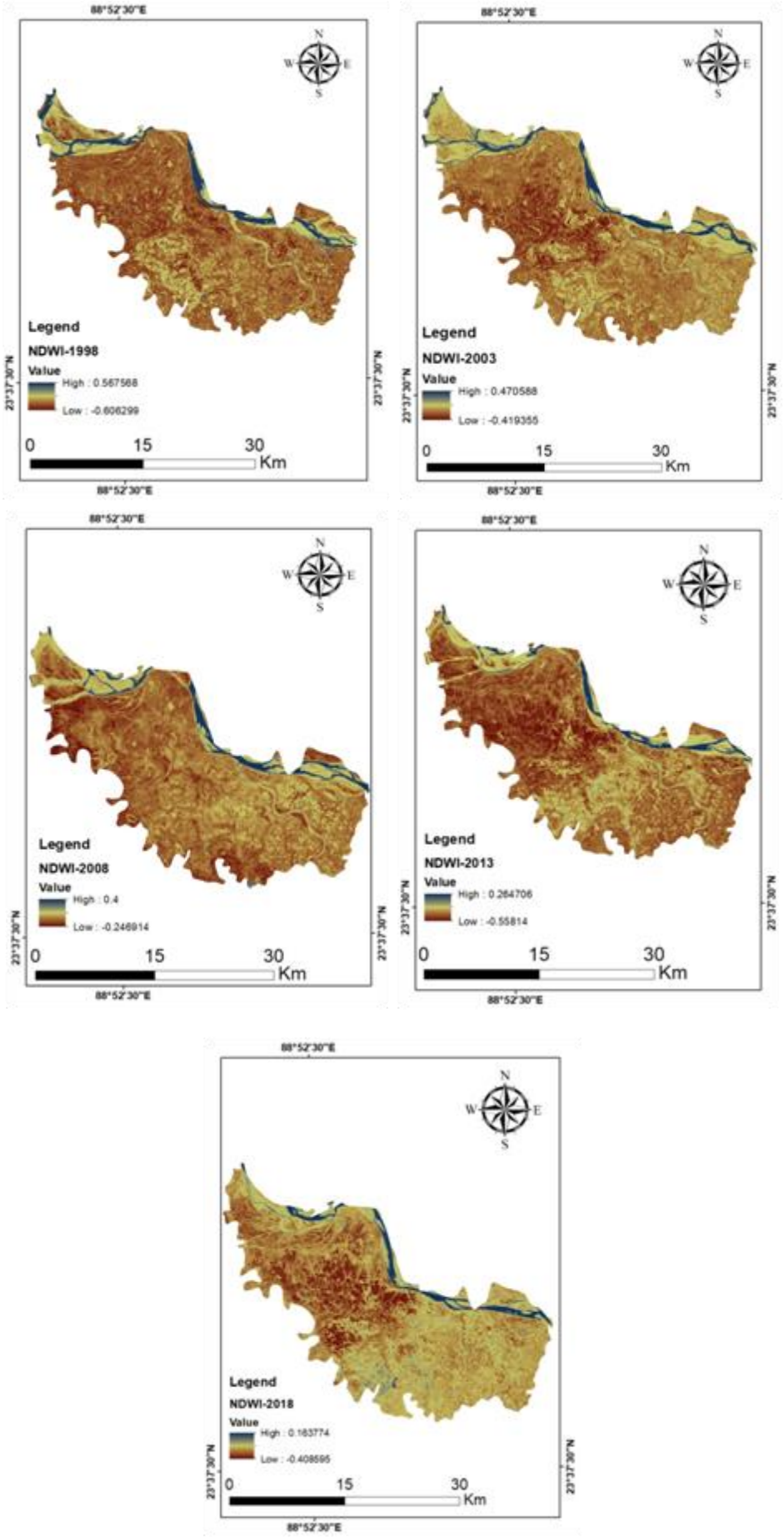

Figure 6 Spatial distribution of NDWI of years 1998, 2003, 2008, 2013 and 2018.

It can also be viewed that the trend of NDWI values was gradually decreasing. Like NDVI, NDWI was maximum in year 1998.Then it followed a gradual trend of subsiding till year 2008. But in 2013, the value of NDWI decreased suddenly (0.264706). And finally in 2018 the value was minimum within the 20 years. NDWI values larger than 0.5 denoted water body and NDWI values less than 0.3 denoted non-water body. Here only in year 1998, the NDWI value was larger than 0.5 and rest while latter showed less than 0.5. From spatial distribution of NDWI, it was found that maximum presence of water body was along the North-East and North-West regions of the district, where vegetation coverage was minimum. This was due to presence of Padma -Gorai-Madhumati river system, as the river system flows through these regions. NDWI value was lower in North-west region (Bheramara and Daulatpur upazilla). From spatial distribution of NDVI, it was found that this area had the maximum vegetation coverage (green color). It was due to the fact that this region over the decades had not undergone through intense urbanization. Also Daulatpur upazilla had a total 6200 acres of land as permanent cropped area and 72700 acres of land as temporary cropped area, comprising almost equaled of Kushtia sadar and Bheramara adjunct. So this area depicted healthy mode vegetation than water body. Along the South-East region of the district, both NDVI and NDWI had moderate values. Kushtia sadar, Meherpur and Kumarkhali upazillas situated in this region were the reason behind the moderate values of DVI and NDWI attributed to rapid growth of urbanization in these upazillas. Kushtia sadar alone faced tremendous augmentation of high rise buildings compacted to the latters. Furthermore, the Bangladesh Water Development Board (BWDB) had extended its irrigation programs in this region (e.g. Ganga-Kobadak irrigation project, the first major irrigation program took place in Bangladesh) over the last decades. As a result, a small amount of water body can be viewed from the spatial distribution of NDWI.

3.4 Interrelation between NDVI, NDWI and LST

Graphical representation of surface covered by vegetation and other type of features in years 1998, 2003, 2008, 2013 and 2018 according to NDVI is displayed in Figure 7. Gaphical representation of surface covered by water-body and other type of features on those years according to NDWI is displayed in Figure 8.

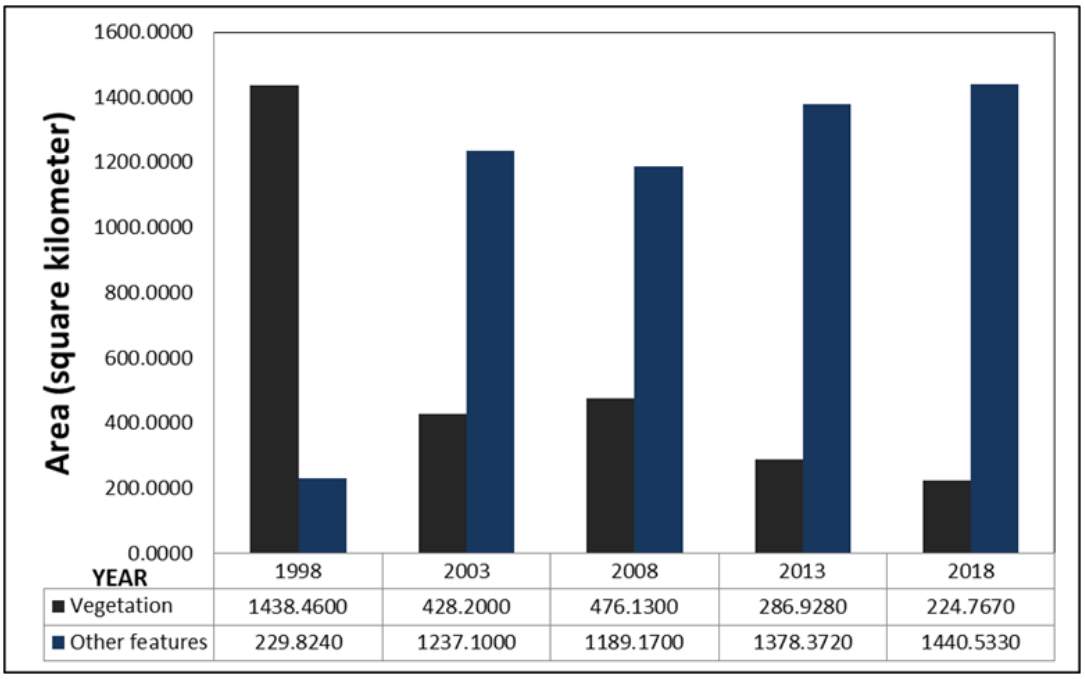

Figure 7 Surface covered by vegetation and other type of features according to NDVI

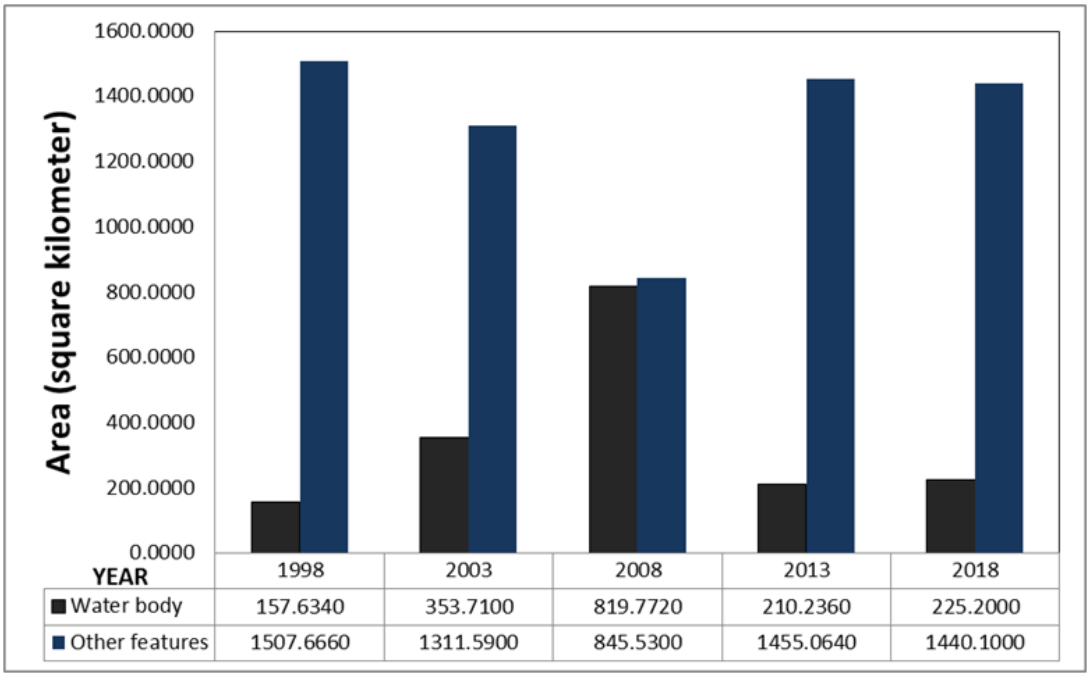

YEAR	1998	2003	2008	2013	2018
Water body	157.6340	353.7100	819.7720	210.2360	225.2000
Other features	1507.6660	1311.5900	845.5300	1455.0640	1440.1000

Figure 8 Surface covered by water body and other type of features according to NDWI

From these two graphs, the drop down of and rise in LST over the following years can be explained. In year 1998, the value of highest LST was 26.4041 ^{0}C and lowest 17.4483 ^{0}C. On that year, the total surface area covered by vegetation was 1438.4600 square kilometers and total surface area covered by water body was 157.6340 square kilometers. So a total of 86.37% of area was covered by vegetation; and in the case of water body, it was only 9.5%. This was the reason behind the low value of highest LST in that year. After 5 years in 2003, the value of highest LST increased to 34.2648 ^{0}C and lowest value was 20.4275 ^{0}C. Both of these LST values were higher than 1998. Now looking back into Figures 7 and 8, it can be concluded that the area with little vegetation cover triggered this temperature rising. The total area covered by vegetation was only 428.2 square kilometer compared to 1438.4600 square kilometers of 1998. Only 25.71% land area was left with vegetation in 2003 (a reduction of 60.66%, with respect to 1998), although the total area covered by water body had increased during these five- year periods, 353.7100 square kilometers. This was as much as 21.24% of the total land area selected for this study. However, it was not enough to mitigate the loss in vegetation cover. As a consequence, LST for 2003 was at its peak. It can be seen that water body was not increased remarkably from 1998 to 2003. So reduced vegetation area had undergone through some urbanization development. Yet, the amount of vegetation cover was replaced by urban region cannot be defined here. Dramatically in year 2008 the highest and lowest values of LST decreased and shaped into a more similar value like 1998. The highest value of LST in year 2008 was 24.9478 ^{0}C and lowest was 17.0759 ^{0}C. From Figure 6, it was observed that land cover due to vegetation was quiet the same to year 2003, 476.1300 square kilometers. But the total area by water body had increased to many fold, 819.7720 square kilometers. This was almost 50% of the total area of Kushtia district. As a result, LST for year 2008 dropped down. So the land area that was not under vegetation coverage in year 2003 had now been replaced by water body in 2008. After 2008, LST again raised at 2013. The values of highest and lowest LST in year 2013 were 33.1100 ^{0}C and 17.9516 ^{0}C respectively. In this year, total area by vegetation cover was half of the year 2008, only 286.9280 square kilometers. And total land coverage by water body decreased devastatingly to 210.2360 square kilometers. So it was found that staggering amount of presence of water body back in year 2008 was not permanent but may be due to some temporary water logging. However in 2018, LST showed a stable value compared to 2013. The highest and lowest values of LST for this year were 32.5918 ^{0}C and 22.013 ^{0}C respectively. Neither the land area by vegetation cover nor by water body had undergone significant changes during these 5 years interval.

From the above discussion, inter relations between LST, NDVI and NDWI is established. Also this study showed that, when maximum area was covered by vegetation and water body during 1998, 2003, 2008, 2013 and 2018, then LST was minimum. Figures 5 and 6 showed the same results and spatial distributions of NDVI and NDWI area during the years considered for study. And in year 2018, most of the land was covered by small vegetation and also LST rose, it indicated vegetation played an important role for dropping LST in the study area. Recent years, cultivation in a land property increased significantly. Generally, rice was produced once but was increased

two times a year now. Extensive use of fertilizer and irrigation had increased the production of a land area, which allowed some of the land area in Bangladesh produce to crops three times a year, even during dry season. The extent of influence of NDVI over LST could be explained more illustratively if statistical reports of Kushtia district of studying years were available.

In this study, other indices Normalized Difference Built-up Index (NDBI) is not included. It is useful for monitoring the spatial distribution and growth of urban built-up areas because they can provide timely and synoptic views of urban land cover. Although the NDBI is useful to map urban built-up areas, it still has some limitations. So for this reason it is not considered in here. At present, urban area is increasing gradually. Most of the area belongs to barren area, crop field, bushes, marsh land, water body and mangrove forests. Barren area is without any covering, like vegetation, acts like desert. In a desert area, massive temperature fluctuation is observed. Temperature rises at a maximum level during day light and it drops to a minimum level at night, in which maximum variation of day and night time temperature is being observed.

4.0 CONCLUSION

LST of Kushtia district had been resoluted based on its "Brightness Temperature and LSE" using Arc-GIS software. The OLI and TIR bands of Landsat 8, Thematic Mapper of Landsat-5 and Enhanced Thematic Mapper of Landsat-7 had been used in this study. The study revealed that the North-East and North-West parts of Kushtia district had less vegetative cover. So LST in these areas are higher than South-East and South-West regions. Following conclusions were drawn from this study:

a) LST may be slightly affected by the water body but this effect was not major over time, because area of large water body changed very slowly;

b) LST can be maintained by increasing vegetation cover; and

c) Even if the vegetation was small bush type or large vegetation under draught condition, it was found to be more affective to reduce LST than bare soil.

From this study, it revealed that total land area by vegetation cover was decreasing in an alarming rate in Kushtia district. If this degradation continued both LST and air temperature could increase in the forthcoming years. Also total land area by water body was also decreasing. However, selecting the middle of the month February (Monsoon season) as study period, the area used to undergo prolong water logging.

Conflict of Interests

The authors declare that there is no conflict of interests regarding the publication of this paper.

Acknowledgement

The authors would like to thank the Khulna University of Engineering & Technology (KUET), Khulna, Bangladesh for providing the financial, logistics and technical support to complete this work.

References

[1] Lu, D., & Weng, Q. (2004). Spectral mixture analysis of the urban landscape in Indianapolis with Landsat ETM+ imagery. Photogrammetric Engineering & Remote Sensing, 70(9), 1053–1062. http://dx.doi.org/10.14358/PERS.70.9.1053

[2] Rajeshwari, A., & Mani, N. D. (2014). Estimation of land surface temperature of Dindigul district using Landsat 8 data. International Journal of Research in Engineering and Technology, 3(5), 122–126. DOI:10.15623/IJRET.2014.0305025

[3] Rahman, H., & Dedieu, G. (1994). SMAC: a simplified method for the atmospheric correction of satellite measurements in the solar spectrum. Remote Sensing, 15(1), 123–143.

[4] Khandelwal, S., Goyal, R., Kaul, N., & Mathew, A. (2018). Assessment of land surface temperature variation due to change in elevation of area surrounding Jaipur, India. The Egyptian Journal of Remote Sensing and Space Science, 21(1), 87–94. https://doi.org/10.1016/j.ejrs.2017.01.005

[5] Mallick, J., Kant, Y., & Bharath, B. D. (2008). Estimation of land surface temperature over Delhi using Landsat-7 ETM+. J. Ind. Geophys. Union, 12(3), 131–140.

[6] Ali, R. R., & Shalaby, A. (2012). Response of topsoil features to the seasonal changes of land surface temperature in the arid environment. *International Journal of Soil Science*, *7*(2), 39–50.
[7] Choudhury, D., Das, K., & Das, A. (2019). Assessment of land use land cover changes and its impact on variations of land surface temperature in Asansol-Durgapur Development Region. The Egyptian Journal of Remote Sensing and Space Science, 22(2), 203-218.
[8] Zullo, F., Fazio, G., Romano, B., Marucci, A., & Fiorini, L. (2019). Effects of urban growth spatial pattern (UGSP) on the land surface temperature (LST): A study in the Po Valley (Italy). Science of The Total Environment, 650, 1740-1751. https://doi.org/10.1016/j.scitotenv.2018.09.331
[9] Zhao, W., Duan, S. B., Li, A., & Yin, G. (2019). A practical method for reducing terrain effect on land surface temperature using random forest regression. Remote sensing of environment, 221, 635-649.
[10] He, J., Zhao, W., Li, A., Wen, F., & Yu, D. (2019). The impact of the terrain effect on land surface temperature variation based on Landsat-8 observations in mountainous areas. International Journal of Remote Sensing, 40(5-6), 1808-1827.
[11] Sobrino, J. A. (1989). Desarrollo de un modelo teórico para implementar la medida de la temperatura realizada mediante teledetección. Aplicación a un campo de naranjos. PhD dissertation, University of Valencia, Valencia, Spain.
[12] Pu, R., Gong, P., Michishita, R., & Sasagawa, T. (2006). Assessment of multi-resolution and multi-sensor data for urban surface temperature retrieval. Remote Sensing of Environment, 104(2), 211–225.
[13] Diak, G. R., & Whipple, M. S. (1995). Note on estimating surface sensible heat fluxes using surface temperatures measured from a geostationary satellite during FIFE 1989. Journal of Geophysical Research: Atmospheres, 100(D12), 25453–25461.
[14] Crago, R., Sugita, M., & Brutsaert, W. (1995). Satellite-derived surface temperatures with boundary layer temperatures and geostrophic winds to estimate surface energy fluxes. Journal of Geophysical Research: Atmospheres, 100(D12), 25447–25451.
[15] Weng, Q., & Fu, P. (2014). Modeling diurnal land temperature cycles over Los Angeles using downscaled GOES imagery. *ISPRS Journal of Photogrammetry and Remote Sensing*, *97*, 78–88.
[16] Hu, L., & Brunsell, N. A. (2013). The impact of temporal aggregation of land surface temperature data for surface urban heat island (SUHI) monitoring. Remote Sensing of Environment, 134, 162–174.
[17] Deng, C., & Wu, C. (2013). A spatially adaptive spectral mixture analysis for mapping subpixel urban impervious surface distribution. Remote Sensing of Environment, 133, 62–70.
[18] Mathew, A., Sreekumar, S., Khandelwal, S., Kaul, N., & Kumar, R. (2016). Prediction of surface temperatures for the assessment of urban heat island effect over Ahmedabad city using linear time series model. Energy and Buildings, 128, 605–616. https://doi.org/10.1016/j.enbuild.2016.07.004
[19] Sinha, S., Sharma, L. K., & Nathawat, M. S. (2015). Improved Land-use/Land-cover classification of semi-arid deciduous forest landscape using thermal remote sensing. The Egyptian Journal of Remote Sensing and Space Science, 18(2), 217–233. https://doi.org/10.1016/j.ejrs.2015.09.005
[20] Pal, S., & Ziaul, S. K. (2017). Detection of land use and land cover change and land surface temperature in English Bazar urban centre. The Egyptian Journal of Remote Sensing and Space Science, 20(1), 125–145. https://doi.org/10.1016/j.ejrs.2016.11.003
[21] Alshaikh, A. Y. (2015). Space applications for drought assessment in Wadi-Dama (West Tabouk), KSA. The Egyptian Journal of Remote Sensing and Space Science, 18(1), S43–S53.
[22] Lisar, S. Y., Motafakkerazad, R., Hossain, M. M., & Rahman, I. M. (2012). Water stress in plants: causes, effects and responses. In Water stress. InTech.
[23] Zhang, H. W., & Huai-Liang, C. H. E. N. (2016). The Application of Modified Normalized Difference Water Index by Leaf Area Index in the Retrieval of Regional Drought Monitoring. DEStech Transactions on Engineering and Technology Research, (sste).
[24] Lambin, E. F. (2001). Global land-use and land-cover change: what have we learned so far? Global Change News, 46, 27-30.
[25] Bhatta, B. (2009). Analysis of urban growth pattern using remote sensing and GIS: a case study of Kolkata, India. International Journal of Remote Sensing, 30(18), 4733-4746.
[26] Griffiths, P., Hostert, P., Gruebner, O., & van der Linden, S. (2010). Mapping megacity growth with multi-sensor data. Remote Sensing of Environment, 114(2), 426-439 https://doi.org/10.1016/j.rse.2009.09.012
[27] Sobrino, J. A., & Raissouni, N. (2000). Toward remote sensing methods for land cover dynamic monitoring: Application to Morocco. International Journal of Remote Sensing, 21(2), 353–366. DOI:10.1080/014311600210876